

# **Modeling Recurrent Safety Critical Events among Commercial Truck Drivers: A Bayesian Hierarchical Jump Power Law Process**

Miao Cai

*Saint Louis University, Saint Louis, MO 63104*

Amir Mehdizadeh

*Auburn University, Auburn, AL 36849*

Qiong Hu

*Auburn University, Auburn, AL 36849*

Mohammad Ali Alamdar Yazdi

*Johns Hopkins University, Baltimore, MD 21202*

Alexander Vinel

*Auburn University, Auburn, AL 36849*

Karen C. Davis

*Miami University, Oxford, OH 45056*

Hong Xian

*Saint Louis University, Saint Louis, MO 63104*

Fadel M. Megahed

*Miami University, Oxford, OH 45056*

Steven E. Rigdon

*Saint Louis University, Saint Louis, MO 63104*

## Abstract

Many transportation safety studies aim to predict crashes based on aggregated road segment data. Safety-critical events (SCEs), such as hard brakes or collision mitigation braking, are widely used as proxy measures of driving risk. While there can only be one crash on a driving shift, multiple SCEs can occur in one shift and they do not interrupt the state of driving. We use data from a large naturalistic driving study that includes over 13 million driving records and 8,386 SCEs generated by 496 commercial truck drivers over one year to address two types of questions regarding the safety behavior of commercial truck drivers. First, does the occurrence of SCEs tend to increase during a shift due to fatigue or some other reason? Second, what is the effect of rest breaks on safety behavior? We propose a Bayesian hierarchical non-homogeneous Poisson process with power law process intensity function and a Bayesian hierarchical jump power law process, similar to the kinds of models that are often applied to analyze failure data from repairable systems. We find that the intensity for hard breaks decreases throughout a shift, and rest breaks reduce the likelihood of having to activate the automated collision mitigation system. Properties of the approach are investigated through a simulation study. Supplementary materials including simulated data and code to obtain parameter estimates for reproducing the work, are available as an online supplement.

*Keywords:* trucking; safety-critical events; reliability; power law process

1

## I. INTRODUCTION

2 Commercial truck drivers “form the lifeblood of [the U.S.] economy” (The White House,  
3 2020), generating annual revenues exceeding \$700 billion from the transportation of 10.8  
4 billion tons of freight (John, 2019). The industry typically requires drivers to be on the road  
5 for an extended period of time, incentivizing drivers with hourly, per-mile or per-delivery  
6 pay schedules. Furthermore, the industry is heavily regulated through the *hours of service*  
7 regulation (Federal Motor Carrier Safety Administration, 2020b), which dictates the total  
8 number of driving hours permitted, minimum length of off-duty rest periods and allowable  
9 weekly total hours of driving/rest. Consequently, a major difference between commercial  
10 (large) truck drivers and commuters is the complex operational environment required of  
11 commercial drivers. Specifically, commercial drivers have to abide by government regulations  
12 while managing industry practices that attempt to optimize both productivity and safety.

13 The safety of truck drivers is of critical importance not only to trucking operators, but  
14 also to the general public. Truck crashes have a two-fold penalty (Tsai et al., 2018) (a) direct  
15 losses arising from injuries, fatalities and property damage affecting the truck driver and other  
16 commuters on the road, and (b) indirect losses in efficiency associated with slowing/damaging  
17 transferred goods and the impact to travel time for other commuters. Alarmingly, despite  
18 the regulatory oversights and continued advancements in safety technologies, the rates of  
19 truck-involved crashes in the U.S. have increased over the past decade. The involvement  
20 rate per 100 million large-truck miles traveled increased from 1.32 in 2008 to 1.48 in 2016  
21 for fatal crashes, and from 21 in 2008 to 31 in 2015, most recent data, for injury crashes  
22 (NHTSA’s National Center for Statistics and Analysis, 2019).

23 Traditional trucking safety studies utilize one or more *road segments* as the unit of analysis  
24 (Mehdizadeh et al., 2020) and attempt to model the occurrence or the number of crashes in a  
25 fixed time period (Lord and Mannering, 2010; Savolainen et al., 2011; Mannering and Bhat,  
26 2014). Thus, the developed models use/resemble a case-control study design (Mehdizadeh  
27 et al., 2020). Limitations of those studies include a small number of observed crashes,  
28 difficulty in selecting control groups, and an undercount of less severe crashes (Mehdizadeh  
29 et al., 2020). More importantly, those studies cannot capture driver behavioral factors which  
30 contribute to 90% of traffic crashes (Federal Highway Administration, 2019).

31 To address the deficiencies in traditional safety studies, large-scale naturalistic driv-  
32 ing studies (NDSs) have received significant attention in recent years (see e.g., Guo, 2019;  
33 Mehdizadeh et al., 2020; Cai et al., 2020). Those studies capitalize on advances in com-  
34 munication, computing and on-board vehicular sensing technologies which have allowed for  
35 the continuous recording of real-world driving data (e.g., timestamps capturing driving lo-  
36 cation, speed, rest brakes, etc.). In addition to their ability to capture continuous data on  
37 possible explanatory variables, NDSs allow for using more frequent near-crash safety critical  
38 events (SCEs) as proxies for crash data. It is well-established that increases in SCEs (e.g.,  
39 hard braking events or the activation of forward-collision mitigation systems) are positively  
40 correlated with crash rates (Dingus et al., 2006; Guo et al., 2010; Gordon et al., 2011; Cai  
41 et al., 2020). Consequently, SCEs are the preferred choice for outcome variables in NDSs  
42 since they are more frequent (Cai et al., 2020) and hence, provide larger statistical power.

43 As with most point process data, SCEs can be divided into models attempting to  
44 (a) quantify the likelihood of observing one or more SCEs through binary classification  
45 (Ghasemzadeh and Ahmed, 2017, 2018) and count data models (Kim et al., 2013), respec-

tively, and (b) estimate the time(s) of observing SCEs (Li et al., 2018; Liu and Guo, 2019; Liu et al., 2019; Guo et al., 2019). Three major limitations are inherent with these modeling approaches. First, NDSs follow drivers/vehicles for an extended time period, i.e., their application resembles a prospective cohort study (Mehdizadeh et al., 2020). However, much of the existing literature utilize methodologies of case-control studies to this type of data by including all events and match them with selective non-events (e.g., Ghasemzadeh and Ahmed, 2018; Das et al., 2019), which reduces the statistical power to detect potentially existing effects and fails to account for the fact that the driving data are nested within drivers. Second, the occurrence of multiple SCEs in an extended time period is not unusual. Therefore, binary classification models are inefficient since they cannot distinguish between cases where one or more SCEs occur. Furthermore, count models fail to consider the time stamps associated with each SCE, which is a critical factor in designing interventions in practice. Third, based on the *hours of service* regulation, breaks are required for intermediate and long trips. The underlying hypothesis/rationale is that these breaks would improve the driver's safety performance, which cannot be modeled using existing methodologies.

Owing to the three identified gaps in NDS models, the overarching motivation of this paper is to examine how large NDS datasets can be modeled to account for both the timing of an observed event and the effect of rest breaks on SCE occurrence. This study is performed in collaboration with a leading shipping freight company in the U.S. The collaboration with industry provides the following unique settings: (a) The company's fleet used a commercially available driving events monitoring system. Both the data management and system maintenance were performed by the company; (b) the truck drivers included in this study were all employed by the company at the time of data collection. The data were collected routinely

69 as a part of their job; and (c) the routes chosen by the drivers are subject to company  
70 policies, delivery windows and government regulations, i.e., naturally follow realistic com-  
71 mercial driving patterns. Based on this setup, we have naturalistic driving data generated  
72 by 496 regional commercial large-truck drivers, capturing over 20 million miles driven and  
73 over 8,300 SCEs. Note that existing trucking NDS datasets are much smaller, with largest  
74 reported values of approximately 200 drivers (Federal Motor Carrier Safety Administration,  
75 2020a) and 0.414 million miles driven (Sparrow et al., 2016). Thus, this study can overcome  
76 the small sample sizes and limited driving locations in previous trucking NDSs.

77 In this article, we address two types of questions regarding the safety behavior of com-  
78 mercial truck drivers. First, does the occurrence of SCEs tend to increase during a shift (a  
79 continuous period for which the driver is on duty, but not necessarily driving), due to fatigue  
80 or some other reason? If so, how is this effect manifested, and for which type of SCE does  
81 this occur? Second, what is the effect of rest breaks on driving safety performance? To what  
82 extent does safety change after a rest break? In order to facilitate the modeling of these two  
83 sets of questions, we introduce and capitalize on the following analogy:

- 84 • The first set of questions can be considered as a degradation process, where contin-  
85 ued driving results in a degraded safety performance similar to continued operation  
86 degrades a process/system in the field of *reliability*.
- 87 • Building on the analogy, a rest-break can be considered as a preventive maintenance  
88 activity, which can be either time-based (e.g., every two hours) or condition-based (e.g.,  
89 if a driver stops for coffee to increase their alertness). The *maintenance* act improves  
90 the driver's reliability by reducing the degradation, which we hypothesize to reduce  
91 the likelihood of an SCE if the occurrence of an SCE is not arbitrary.

92     • A potential difference between a product and a driver's reliability is that products  
 93        of similar vintage are typically assumed to be homogeneous. On the other hand, the  
 94        modeling of drivers should be personalized (i.e., assuming heterogeneity of the sampling  
 95        units), which can be accounted for using hierarchical modeling approaches.  
 96        With the research questions and analogy in mind, we introduce a Bayesian hierarchi-  
 97        cal non-homogeneous Poisson process with the power law process (PLP) intensity function  
 98        to model SCEs within shifts. This model can account for driver-level unobserved hetero-  
 99        geneity by specifying driver-level random intercepts for the rate parameter in PLP. On the  
 100        other hand, to account for the feature that multiple breaks are nested within a shift among  
 101        commercial truck drivers, we then propose a Bayesian hierarchical jump power law process  
 102        (JPLP) to take potential reliability changes at the time of rests into consideration. Figure 1  
 103        presents an illustration of using PLP and JPLP in modeling the intensity function of SCEs.

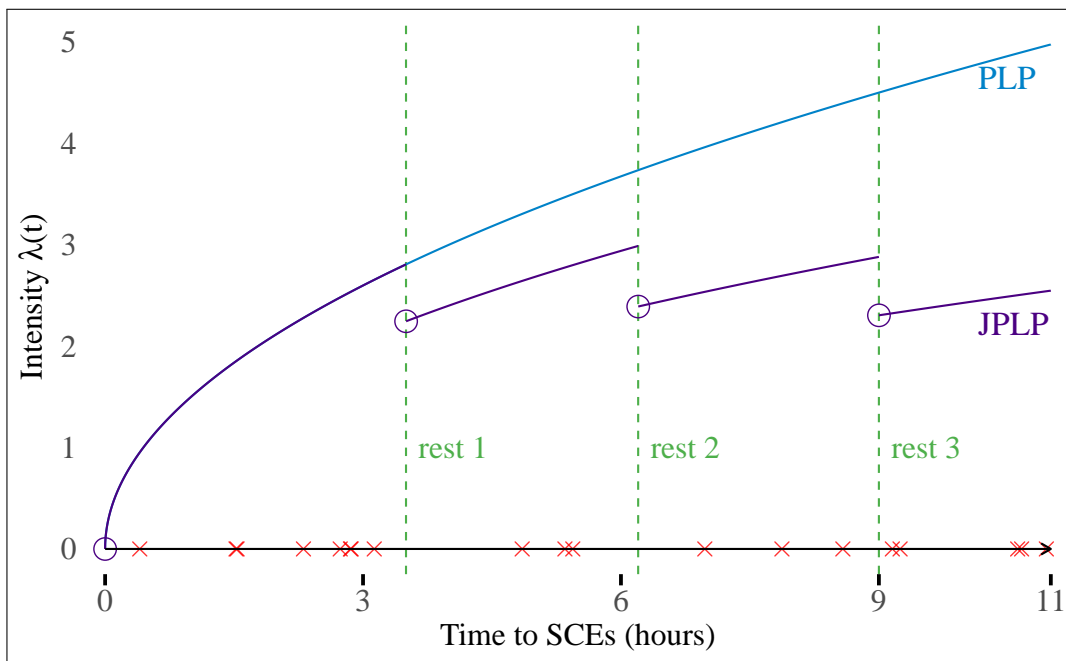


Figure 1: An illustration of a simulated intensity function of PLP and JPLP. The  $x$ -axis shows time in hours since start and  $y$ -axis shows the intensity of SCEs. The crosses mark the time to SCEs and the vertical dotted lines indicates the time of the rests.

104 The structure of this article is as follows. In Section II, we define our terminology  
105 and notation for shifts, segments, and events for naturalistic driving data generated by  
106 commercial truck drivers. In Section III, we specify our proposed PLP and JPLP models,  
107 their intensity functions and likelihood functions. In section IV, we present the results of real  
108 data analyses for 496 commercial truck drivers using PLP and JPLP. In Section V, simulation  
109 studies are conducted to demonstrate the validity of our code and the consequences if the  
110 models are not specified correctly. In Section VI, strengths, possible limitations, and future  
111 research directions are discussed. In the Appendix, two maps of our ping data and trace plots  
112 of selected parameters are supplied. A simulated data set, description on data structure,  
113 and Stan and R code for Bayesian PLP and JPLP estimation are provided in the online  
114 supplementary material.

## 115 II. TERMINOLOGY AND NOTATION

116 Figure 2 presents a time series plot of speed data for a sample truck driver (including two  
117 shifts and six segments nested within the shifts) and arrows suggesting shifts and segments.  
118 We use  $d = 1, 2, \dots, D$  as the index for different drivers. A shift  $s = 1, 2, \dots, S_d$  is on-duty  
119 periods with no breaks longer than 10 hours for driver  $d$ . Per the *hours of service* regulations  
120 (Federal Motor Carrier Safety Administration, 2020b), a shift must be no more than 14 hours  
121 with no more than 11 hours of driving. This leads to the phenomena that multiple segments  
122  $r = 1, 2, \dots, R_{d,s}$  are separated by breaks longer than 30 minutes but less than 10 hours for  
123 each driver  $d$  and shift  $s$ .

124 SCEs can occur any time in the segments whenever preset kinematic thresholds are  
125 triggered while driving. We use  $i = 1, 2, \dots, I_{d,s}$  as the index for the  $i$ -th SCE for driver  $d$

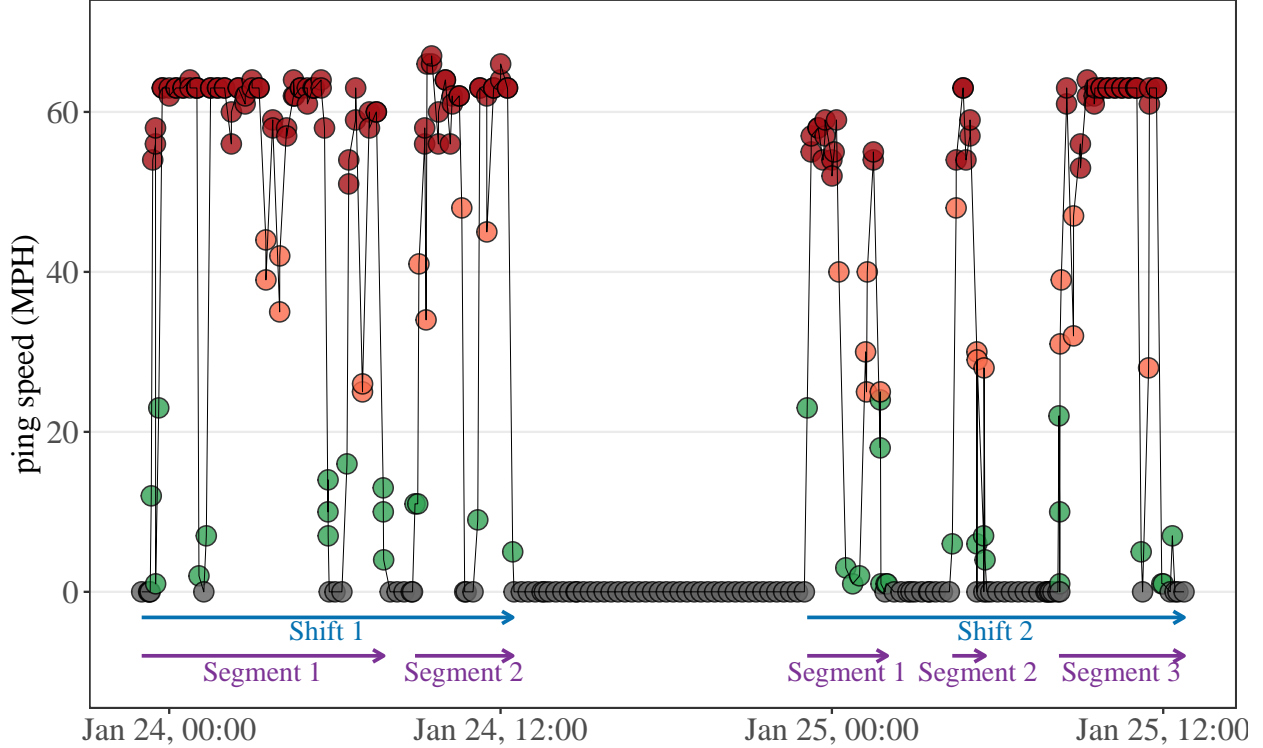


Figure 2: Time series plot of naturalistic truck driving sample ping data (points) and the aggregation process from pings to shifts and segments (arrows).

in shift  $s$ . For each SCE,  $t_{d,s,i}$  is the time to the  $i$ -th SCE for driver  $d$  measured from the beginning of the  $s$ -shift and the rest times between segments are excluded from calculation.  $n_{d,s,r}$  is the number of SCEs for segment  $r$  within shift  $s$  for driver  $d$ .  $a_{d,s,r}$  is the end time of segment  $r$  within shift  $s$  for driver  $d$ .

130

### III. MODELS

#### 131 A. Non-homogeneous Poisson Process (NHPP) and Power Law Process

132 We assume the times to SCEs  $t$  follow a non-homogeneous Poisson process, whose intensity function  $\lambda(t)$  is non-constant, having the functional form

$$\lambda_{PLP}(t) = \frac{\beta}{\theta} \left( \frac{t}{\theta} \right)^{\beta-1}, \quad (1)$$

134 where the shape parameter  $\beta$  indicates reliability improvement ( $\beta < 1$ ), constant ( $\beta = 1$ ), or  
 135 deterioration ( $\beta > 1$ ), and the scale parameter  $\theta$  determines the rate of events. We assume  
 136 the intensity function of a power law process since it is an established model (Rigdon and  
 137 Basu, 1989, 2000) with a flexible functional form and allows for relatively simple inference.

138 B. Bayesian Hierarchical Power Law Process (PLP)

139 The Bayesian hierarchical power law process is parameterized as:

$$\begin{aligned}
 t_{d,s,1}, t_{d,s,2}, \dots, t_{d,s,n_{d,s}} &\sim \text{PLP}(\beta, \theta_{d,s}, \tau_{d,s}) \\
 \log \theta_{d,s} &= \gamma_{0d} + \gamma_1 x_{d,s,1} + \gamma_2 x_{d,s,2} + \dots + \gamma_k x_{d,s,k} \\
 \gamma_{01}, \gamma_{02}, \dots, \gamma_{0D} &\sim \text{i.i.d. } N(\mu_0, \sigma_0^2),
 \end{aligned} \tag{2}$$

140 where  $t_{d,s,i}$  is the time to the  $i$ -th event for driver  $d$  in shift  $s$ ,  $\tau_{d,s} = a_{d,s,R_{d,s}}$  is the length  
 141 of time of shift  $s$  (truncation time) for driver  $d$ , and  $n_{d,s} = \sum_{r=1}^{n_{d,s}}$  is the number of SCEs in  
 142 shift  $s$  for driver  $d$ . The priors for the parameters and hyperparameters are taken to be the  
 143 relatively non-informative distributions

$$\begin{aligned}
 \beta &\sim \text{Gamma}(1, 1) \\
 \gamma_1, \gamma_2, \dots, \gamma_k &\sim \text{i.i.d. } N(0, 10^2) \\
 \mu_0 &\sim N(0, 5^2) \\
 \sigma_0 &\sim \text{Gamma}(1, 1).
 \end{aligned} \tag{3}$$

144 The likelihood function of event times generated from a PLP for driver  $d$  in shift  $s$  can

<sup>145</sup> be formulated based on Rigdon and Basu (2000, p. 60) as

$$L_{d,s}(\beta, \gamma_{0d}, \gamma | \mathbf{X}_d, \mathbf{W}_s) = \left( \prod_{i=1}^{n_{d,s}} \lambda_{\text{PLP}}(t_{d,s,i}) \right) \exp\left(- \int_0^{\tau_{d,s}} \lambda_{\text{PLP}}(u) du\right)$$

$$= \begin{cases} \exp\left(-(\tau_{d,s}/\theta_{d,s})^\beta\right), & \text{if } n_{d,s} = 0, \\ \left( \prod_{i=1}^{n_{d,s}} \beta \theta_{d,s}^{-\beta} t_{d,s,i}^{\beta-1} \right) \exp\left(-(\tau_{d,s}/\theta_{d,s})^\beta\right), & \text{if } n_{d,s} > 0, \end{cases} \quad (4)$$

<sup>146</sup> where  $\mathbf{X}_d$  indicates driver specific variables (e.g. driver age and gender),  $\mathbf{W}_s$  represents

<sup>147</sup> shift specific variables (e.g. precipitation and traffic), and  $\theta_{d,s}$  is the function of parameters

<sup>148</sup>  $\gamma_{0d}, \gamma_1, \gamma_2, \dots, \gamma_k$  and variables  $x_{d,s,1}, x_{d,s,2}, \dots, x_{d,s,k}$  given in the third line of Equation (2).

<sup>149</sup> The full likelihood function for all drivers can be computed using:

$$L = \prod_{d=1}^D \prod_{s=1}^{S_d} L_{d,s}(\beta, \gamma_{0d}, \gamma | \mathbf{X}_d, \mathbf{W}_s) \quad (5)$$

<sup>150</sup> where  $L_{d,s}(\beta, \gamma_{0d}, \gamma | \mathbf{X}_d, \mathbf{W}_s)$  is provided in Equation (4). Models like this are often used in

<sup>151</sup> the literature for repairable systems reliability (Rigdon and Basu, 2000). Here, a “failure”

<sup>152</sup> can be thought of as the occurrence of a SCE.

### <sup>153</sup> C. Bayesian Hierarchical Jump Power Law Process (JPLP)

<sup>154</sup> Since the Bayesian hierarchical PLP does not account for rest breaks ( $r = 1, 2, \dots, R_{d,s}$ )

<sup>155</sup> within shifts and associated potential performance improvement, we propose a Bayesian hi-

<sup>156</sup> erarchical JPLP with an additional jump parameter  $\kappa$ . Our proposed JPLP has the following

<sup>157</sup> piece-wise intensity function:

$$\lambda_{\text{JPLP}}(t|d, s, r, \beta, \gamma_{0d}, \gamma, \mathbf{X}_d, \mathbf{W}_s) =$$

$$\begin{cases} \kappa^0 \lambda(t|\beta, \gamma_{0d}, \gamma, \mathbf{X}_d, \mathbf{W}_s), & 0 < t \leq a_{d,s,1}, \\ \kappa^1 \lambda(t|\beta, \gamma_{0d}, \gamma, \mathbf{X}_d, \mathbf{W}_s), & a_{d,s,1} < t \leq a_{d,s,2}, \\ \vdots & \vdots \\ \kappa^{R-1} \lambda(t|\beta, \gamma_{0d}, \gamma, \mathbf{X}_d, \mathbf{W}_s), & a_{d,s,R-1} < t \leq a_{d,s,R}, \end{cases} \quad (6)$$

$$= \kappa^{r-1} \lambda(t|d, s, r, \kappa, \beta, \gamma_{0d}, \gamma, \mathbf{X}_d, \mathbf{W}_s), \quad a_{d,s,r-1} < t \leq a_{d,s,r},$$

<sup>158</sup> where the introduced parameter  $\kappa$  is the amount of intensity function change once the driver  
<sup>159</sup> takes a break, and  $a_{d,s,r}$  is the end time of segment  $r$  within shift  $s$  for driver  $d$ . By definition,  
<sup>160</sup> the end time of the zero-th segment  $a_{d,s,0} = 0$ , and the end time of the last segment for the  
<sup>161</sup>  $d$ -driver within the  $s$ -th shift  $a_{d,s,R_{d,s}}$  equals the shift end time  $\tau_{d,s}$ . We assume that this  $\kappa$   
<sup>162</sup> is constant across drivers and shifts.

<sup>163</sup> The Bayesian hierarchical JPLP model is parameterized as:

$$t_{d,s,1}, t_{d,s,2}, \dots, t_{d,s,n_{d,s}} \sim \text{JPLP}(\beta, \theta_{d,s}, \tau_{d,s}, \kappa)$$

$$\log \theta_{d,s} = \gamma_{0d} + \gamma_1 x_{d,s,1} + \gamma_2 x_{d,s,2} + \dots + \gamma_k x_{d,s,k} \quad (7)$$

$$\gamma_{01}, \gamma_{02}, \dots, \gamma_{0D} \sim \text{i.i.d. } N(\mu_0, \sigma_0^2).$$

<sup>164</sup> With the exception of the  $\kappa$  parameter, the above formulation is identical with that presented  
<sup>165</sup> in Equation (2). We set the prior distribution for  $\kappa$  as uniform(0, 2), which allows the  
<sup>166</sup> intensity function to change by a factor that ranges from 0 to 2 at rest breaks. The priors

<sup>167</sup> and hyperpriors for the JPLP are assigned as

$$\beta \sim \text{Gamma}(1, 1)$$

$$\kappa \sim \text{Uniform}(0, 2)$$

$$\gamma_1, \gamma_2, \dots, \gamma_k \sim \text{i.i.d. } N(0, 10^2) \quad (8)$$

$$\mu_0 \sim N(0, 5^2)$$

$$\sigma_0 \sim \text{Gamma}(1, 1).$$

<sup>168</sup> The likelihood function of event times generated from a JPLP for driver  $d$  on shift  $s$  is

<sup>169</sup> defined as:

$$L_{d,s}^*(\kappa, \beta, \gamma_{0d}, \gamma | \mathbf{X}_d, \mathbf{W}_s) = \begin{cases} \left( \prod_{i=1}^{n_{d,s}} \lambda_{\text{JPLP}}(t_{d,s,i}) \right) \exp\left(-\int_0^{\tau_{d,s}} \lambda_{\text{JPLP}}(u) du\right) \\ \left\{ \begin{array}{ll} \exp\left(-\int_0^{\tau_{d,s}} \lambda_{\text{JPLP}}(u) du\right), & \text{if } n_{d,s} = 0, \\ \left( \prod_{i=1}^{n_{d,s}} \lambda_{\text{JPLP}}(t_{d,s,i}) \right) \exp\left(-\int_0^{\tau_{d,s}} \lambda_{\text{JPLP}}(u) du\right), & \text{if } n_{d,s} > 0, \end{array} \right. \end{cases} \quad (9)$$

<sup>170</sup> where the piecewise intensity function  $\lambda_{\text{JPLP}}(t_{d,s,i})$  is given in Equation (6). Since the inten-

<sup>171</sup> sity function depends on the segment  $r$  for a given driver  $d$  on shift  $s$ , it is easier to present

<sup>172</sup> the likelihood function at a segment level, which can be computed as

$$L_{d,s,r}^*(\kappa, \beta, \gamma_{0d}, \gamma | \mathbf{X}_d, \mathbf{W}_r) = \begin{cases} \exp\left(-\int_{a_{d,s,r-1}}^{a_{d,s,r}} \lambda_{\text{JPLP}}(u) du\right), & \text{if } n_{d,s,r} = 0, \\ \left( \prod_{i=1}^{n_{d,s,r}} \lambda_{\text{JPLP}}(t_{d,s,r,i}) \right) \exp\left(-\int_{a_{d,s,r-1}}^{a_{d,s,r}} \lambda_{\text{JPLP}}(u) du\right), & \text{if } n_{d,s,r} > 0, \end{cases} \quad (10)$$

<sup>173</sup> where the intensity function  $\lambda_{\text{JPLP}}$  is fixed for driver  $d$  on shift  $s$  and segment  $r$ ,  $t_{d,s,r,i}$  denotes

<sup>174</sup> the time to the  $i^{th}$  SCE for driver  $d$  on shift  $s$  and segment  $r$  measured from the beginning

175 of the shift, and  $n_{d,s,r}$  is the number of SCEs for driver  $d$  on shift  $s$  and segment  $r$ .

176 Compared to the PLP likelihood function given in Equation (5) where  $\mathbf{W}_s$  are assumed  
177 to be fixed numbers during an entire shift, the rewritten likelihood function for JPLP in  
178 Equation (10) assumes that the external covariates  $\mathbf{W}_r$  vary between different segments in  
179 a shift. In this way, the JPLP can account for the variability between different segments  
180 within a shift. Therefore, the overall likelihood function for drivers  $d = 1, 2, \dots, D$ , their  
181 corresponding shifts  $s = 1, 2, \dots, S_d$ , and segments  $r = 1, 2, \dots, R_{d,s}$  can be computed as

$$L^* = \prod_{d=1}^D \prod_{s=1}^{S_d} \prod_{r=1}^{R_{d,s}} L_{d,s,r}^*, \quad (11)$$

182 where  $L_{d,s,r}^*$  is a likelihood function given in Equation (10), in which the intensity function  
183  $\lambda_{\text{JPLP}}$  has a fixed functional form provided in the last line of Equation (6) for a certain driver  
184  $d$  in a given shift  $s$  and segment  $r$ .

185 IV. REAL DATA ANALYSIS

186 A. Data description

187 A naturalistic truck driving data set was provided by a large national commercial trucking  
188 company in North America. The data set includes 496 regional drivers who move freights  
189 in regional routes that may include several surrounding states. A total of 13,187,289 ping  
190 records were generated between April 2015 and March 2016, with a total traveled distance of  
191 20,042,519 miles in 465,641 hours (average speed 43 miles per hour). Each ping records the  
192 date and time (year, month, day, hour, minute, and second), latitude and longitude (specific  
193 to five decimal places), driver identification number, and speed at that time point. Figures  
194 4a and 4b in Appendix A. show the geographic distribution of the active and inactive pings.

195 The two maps suggest that most of the sample pings closely match the population density  
196 distribution in the United States. These pings were then aggregated into 64,860 shifts and  
197 180,408 segments.

198 In addition, 8,386 kinematic SCEs were captured from a popular, commercial sensor-  
199 based system independent of the pings, including 3,941 (47%) headway, 3,576 (42.6%) hard  
200 brakes, and 869 (10.4%) collision mitigation. The three types of SCEs in this study are  
201 identical with those used in Cai et al. (2020), and the association between crashes and these  
202 SCEs have been established. The definitions and thresholds of these SCEs are as follows:

203 I copy-paste the following list from our TRC paper, need to change the wording to avoid  
204 plagiarism

- 205 • Headway, which signals an instance of tailgating for at least 118 seconds at an unsafe  
206 gap time (a measure of distance between leading and trailing vehicles) of 2.8 seconds  
207 or less (Grove et al., 2015).
- 208 • Hard brakes, which are defined as instances of a deceleration rate of 9.5 miles per hour  
209 per second or more.
- 210 • Activation of the forward collision mitigation system.

211 Historic weather data, including precipitation probability, precipitation intensity, and  
212 wind speed, were queried from the DarkSky Application Programming Interface, which pro-  
213 vides historic real-time and hour-by-hour nationwide historic weather conditions for spe-  
214 cific latitude-longitude-date-time combinations (The Dark Sky Company, LLC, 2020). The  
215 weather data were then merged back to the ping data set and aggregated to shift- and  
216 segment-level by taking the mean. Table 1 present the summary statistics of the driver-,  
217 shift-, segment-level variables in our data set.

Table 1: Summary statistics of driver-, shift-, and segment-level variables

Variable	Statistics
Median [IQR] of <i>driver</i> -level variables (N = 496)	
Age	47 [36, 55]
Race (N (percent))	
White	246 (49.6%)
Black	206 (41.5%)
Other	44 ( 8.9%)
Male	460 (92.7%)
Distance	34422.9 [13707.5, 68660.9]
Driving hours	808.1 [337.8, 1626.4]
Mean speed	43.1 [40.8, 44.7]
Mean (S.D.) of <i>shift</i> -level variables (N = 64,860)	
Speed S.D.	22.6 (4.3)
Preci. intensity	0.0 (0.0)
Preci. prob.	0.1 (0.2)
Wind speed	3.6 (2.5)
Mean (S.D.) of <i>segment</i> -level variables (N = 180,408)	
Speed S.D.	18.6 (7.8)
Preci. intensity	0.0 (0.0)
Preci. prob.	0.1 (0.2)
Wind speed	3.6 (2.9)

IQR: interquartile range; S.D.: standard deviation;

Preci. intensity: precipitation intensity;

Precip. prob.: precipitation probability.

218 B. Real data analysis results

219 We applied the hierarchical Bayesian PLP and JPLP models to this data as specified in  
 220 Equations (2) and (7). Since we have several types of SCEs, we then applied the JPLP to  
 221 the three different types of SCEs separately. Samples of the posterior distributions were  
 222 drawn using the probabilistic programming language Stan in R (Carpenter et al., 2017; Stan  
 223 Development Team, 2018). The convergence of Hamiltonian Monte Carlo was checked using  
 224 Gelman-Rubin diagnostic statistics  $\hat{R}$  (Gelman et al., 1992), effective sample size (ESS), and  
 225 trace plots.

226 Table 2 presents the posterior mean, 95% credible interval (CI), Gelman-Rubin diagnostic  
 227 statistics  $\hat{R}$ , and ESS for the sample 496 regional drivers using PLP and JPLP. In both the

228 PLP and JPLP models, the posterior means of the shape parameters  $\beta$  are less than one  
 229 and the 95% credible intervals exclude one, indicating SCEs occur in the early stages of the  
 230 shifts. In the JPLP, the reliability jump parameter  $\kappa$  was close to 1, suggesting that within  
 231 a shift, rests have very minor effects on the intensity of SCEs.

232 Figure 3, which gives histograms for estimates of the random intercepts, indicates that  
 233 there is considerable variability across drivers. The random intercepts  $\gamma_{0d}$  are on average  
 234 larger in the JPLP model than those in the PLP model, while variability of random intercepts  
 235 is similar in the two models. These patterns are consistent with the parameter estimates of  
 236  $\mu_0$  and  $\sigma_0$  in Table 2. All the Gelman-Rubin diagnostic statistics  $\hat{R}$  are less than 1.1 and the  
 237 ESSs are greater than 1,000. The trace plots (Figure 5) of important variables  $(\beta, \kappa, \mu_0, \sigma_0)$   
 238 given in Appendix B. indicate that all four chains for the parameters are well mixed. All  
 239 these evidence suggests that a steady state posterior distribution have been reached for the  
 240 two models.

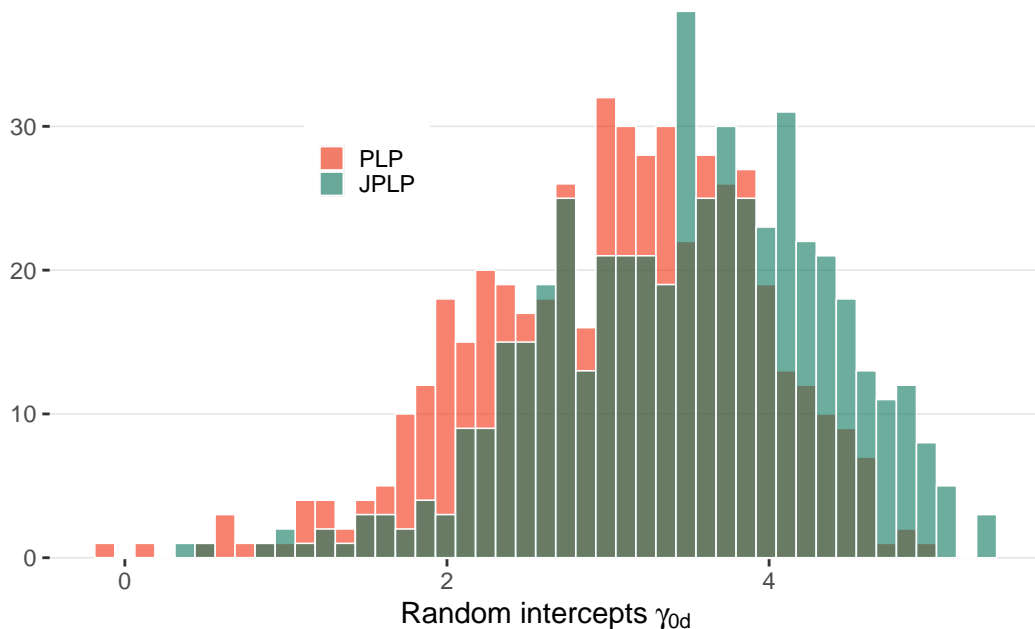


Figure 3: Histogram of random intercepts  $\gamma_{0d}$  across the 496 drivers.

Table 2: Posterior mean, 95% credible interval, Rhat, and effective sample size (ESS) of PLP and JPLP models for 496 commercial truck drivers

Parameters	Power law process				Jump power law process			
	mean	95% CI	$\hat{R}$	ESS	mean	95% CI	$\hat{R}$	ESS
$\hat{\beta}$	0.968	( 0.948, 0.988)	1.000	6,500	0.962	( 0.940, 0.985)	1.001	3,798
$\hat{\kappa}$					1.020	( 0.995, 1.045)	1.000	5,400
$\hat{\mu}_0$	3.038	( 2.397, 3.688)	1.001	2,979	3.490	( 2.899, 4.091)	1.001	3,079
$\hat{\sigma}_0$	0.974	( 0.897, 1.058)	1.000	9,581	0.982	( 0.905, 1.066)	1.000	9,050
Age	0.003	(-0.005, 0.012)	1.001	2,250	0.004	(-0.005, 0.012)	1.001	2,566
Race: black	-0.113	(-0.329, 0.103)	1.002	1,951	-0.130	(-0.342, 0.087)	1.001	2,277
Race: other	-0.343	(-0.707, 0.021)	1.001	2,833	-0.361	(-0.729, 0.010)	1.001	3,334
Gender: female	-0.071	(-0.441, 0.300)	1.001	3,069	-0.071	(-0.435, 0.296)	1.001	4,162
Mean speed	0.019	( 0.016, 0.023)	1.000	20,229	0.015	( 0.013, 0.018)	1.000	19,827
Speed variation	0.026	( 0.017, 0.034)	1.000	24,825	0.017	( 0.013, 0.022)	1.000	13,127
Preci. intensity	-3.608	(-6.181, -0.935)	1.000	22,025	-2.136	(-3.785, -0.368)	1.000	24,397
Preci. prob.	0.397	( 0.168, 0.628)	1.000	21,416	0.121	(-0.050, 0.296)	1.000	25,329
Wind speed	0.018	( 0.008, 0.029)	1.000	32,980	0.010	( 0.001, 0.018)	1.000	33,093

95% CI: 95% credible interval; ESS: effective sample size;

PLP: power law process; JPLP: jump power law process;

Preci. intensity: precipitation intensity; Precip. prob.: precipitation probability.

We further estimated the JPLP models for different types of SCEs (headway, hard brakes, and collision mitigation) separately, and the results are presented in Table 3. Headway and hard brakes are similar: the posterior means and 95% credible intervals for parameters  $\beta$  and  $\kappa$  are nearly identical, although the hyperparameters for random intercepts are quite different. The results that  $\hat{\beta} < 1$  and  $\hat{\kappa} > 1$  suggest that headway and hard brake tend to occur in the early stages of driving shifts, and taking short breaks will slightly increase the intensity of these two events, although the credible intervals contain 1. In contrast, collision mitigation show a different pattern: they tend to occur in later stages of driving shifts, and taking short breaks will reduce the intensity of the event. The variability estimate of random intercepts across drivers ( $\sigma_0$ ) is stronger for headway than hard brake, and collision mitigation.

Table 3: Parameter estimates and 95% credible intervals for jump power law process on 496 truck drivers, stratified by different types of safety-critical events

Parameters	Headway	Hard brake	Collision mitigation
$\hat{\beta}$	0.989 ( 0.956, 1.023)	0.922 ( 0.889, 0.955)	1.020 ( 0.950, 1.096)
$\hat{\kappa}$	1.034 ( 0.998, 1.071)	1.034 ( 0.996, 1.072)	0.890 ( 0.821, 0.964)
$\hat{\mu}_0$	7.096 ( 6.083, 8.139)	3.470 ( 2.770, 4.199)	4.729 ( 3.836, 5.666)
$\hat{\sigma}_0$	1.564 ( 1.411, 1.730)	1.073 ( 0.973, 1.182)	0.922 ( 0.786, 1.074)
Age	-0.006 (-0.020, 0.009)	0.011 ( 0.001, 0.021)	0.002 (-0.009, 0.012)
Race: black	0.184 (-0.170, 0.546)	-0.312 (-0.565, -0.064)	0.113 (-0.153, 0.386)
Race: other	0.306 (-0.340, 0.967)	-0.539 (-0.968, -0.106)	0.100 (-0.373, 0.605)
Gender: female	0.266 (-0.343, 0.870)	-0.217 (-0.654, 0.230)	-0.181 (-0.675, 0.309)
Mean speed	-0.026 (-0.031, -0.021)	0.043 ( 0.039, 0.047)	0.039 ( 0.032, 0.046)
Speed variation	-0.009 (-0.017, -0.002)	0.017 ( 0.010, 0.024)	0.013 (-0.002, 0.027)
Preci. intensity	-0.771 (-4.306, 3.188)	-1.912 (-3.924, 0.269)	-0.676 (-6.329, 6.297)
Preci. prob.	0.694 ( 0.376, 1.015)	-0.495 (-0.724, -0.263)	0.808 ( 0.206, 1.423)
Wind speed	0.003 (-0.009, 0.015)	0.019 ( 0.005, 0.034)	0.000 (-0.025, 0.026)

Preci. intensity: precipitation intensity; Precip. prob.: precipitation probability.

252

## V. SIMULATION STUDY

253 A. Simulation setting

254 We conducted a simulation study to evaluate the performance of our proposed NHPP and

255 JPLP under different simulation scenarios. We performed 1,000 simulations to each of the

256 following three scenarios with different number of drivers  $D = 10, 25, 50, 75, 100$ :

257 1. Data generated from a PLP and estimated assuming a PLP (PLP),

258 2. Data generated from a JPLP and estimated assuming a JPLP (JPLP),

259 3. Data generated from a JPLP, but estimated assuming a PLP (PLP  $\leftarrow$  JPLP).

260 Specifically, for each driver, the number of shifts is simulated from a Poisson distribution

261 with the mean parameter of 10. We assume there are three predictor variables  $x_1, x_2, x_3$  for

262  $\theta$  ( $k = 3$ ).  $x_1, x_2, x_3$  and the shift time  $\tau_{d,s}$  are generated from the following process:

$$\begin{aligned} x_1 &\sim \text{Normal}(1, 1^2) \\ x_2 &\sim \text{Gamma}(1, 1) \\ x_3 &\sim \text{Poisson}(2) \\ \tau_{d,s} &\sim \text{Normal}(10, 1.3^2) \end{aligned} \tag{12}$$

263 The parameters and hyperparameters are assigned the following values or generated from  
264 the following process:

$$\begin{aligned} \mu_0 &= 0.2, \sigma_0 = 0.5, \\ \gamma_{01}, \gamma_{02}, \dots, \gamma_{0D} &\sim \text{i.i.d. } N(\mu_0, \sigma_0^2) \\ \gamma_1 &= 1, \gamma_2 = 0.3, \gamma_3 = 0.2 \\ \theta_{d,s} &= \exp(\gamma_{0d} + \gamma_1 x_1 + \gamma_2 x_2 + \gamma_3 x_3) \\ \beta &= 1.2, \kappa = 0.8. \end{aligned} \tag{13}$$

265 After the predictor variables, shift time, and parameters are generated, the time to events  
266 are generated from either the PLP or the JPLP.

267 The parameters are then estimated using the likelihood functions given in Equations (5)  
268 and (11) using the probabilistic programming language **Stan** in R (Carpenter et al., 2017;  
269 Stan Development Team, 2018), which uses efficient Hamiltonian Monte Carlo to sample from  
270 the posterior distributions. For each simulation, one chain is applied, with 2,000 warmup  
271 and 2,000 post-warmup iterations drawn from the posterior distributions.

<sup>272</sup> B. Simulation results

<sup>273</sup> The simulation results are shown in Table 4. For the five sets of drivers  $D = 10, 25, 50, 75, 100$   
<sup>274</sup> in each of the three scenarios, mean of estimation bias  $\Delta = \hat{\mu} - \mu$ , and mean of standard  
<sup>275</sup> error estimates for parameters  $\beta, \kappa, \gamma_1, \gamma_2, \gamma_3$  and hyperparameters  $\mu_0$  and  $\sigma$  are calculated.

Table 4: Biases  $\Delta$  and standard errors (S.E.) for PLP, JPLP, and  $\text{PLP} \leftarrow \text{JPLP}$  simulation results

Scenario	D	estimate	$\beta$	$\kappa$	$\mu_0$	$\sigma_0$	$\gamma_1$	$\gamma_2$	$\gamma_3$
PLP	10	bias $\Delta$	-0.0102		-0.0282	0.0527	0.0203	0.0095	0.0067
PLP	25	bias $\Delta$	-0.0045		-0.0015	0.0220	0.0066	0.0046	0.0012
PLP	50	bias $\Delta$	-0.0017		-0.0068	0.0077	0.0040	0.0033	0.0005
PLP	75	bias $\Delta$	-0.0017		-0.0026	0.0091	0.0034	0.0004	0.0007
PLP	100	bias $\Delta$	-0.0006		-0.0034	0.0042	0.0009	0.0009	0.0003
PLP	10	S.E.	0.0589		0.2401	0.1722	0.0777	0.0696	0.0413
PLP	25	S.E.	0.0360		0.1392	0.0916	0.0459	0.0414	0.0247
PLP	50	S.E.	0.0254		0.0960	0.0610	0.0316	0.0286	0.0172
PLP	75	S.E.	0.0207		0.0784	0.0497	0.0258	0.0232	0.0139
PLP	100	S.E.	0.0179		0.0667	0.0420	0.0220	0.0198	0.0119
JPLP	10	bias $\Delta$	-0.0226	0.0149	-0.0401	0.0696	0.0331	0.0218	0.0092
JPLP	25	bias $\Delta$	-0.0131	0.0084	-0.0202	0.0219	0.0158	0.0081	0.0039
JPLP	50	bias $\Delta$	-0.0057	0.0032	0.0014	0.0111	0.0037	0.0012	0.0039
JPLP	75	bias $\Delta$	-0.0058	0.0028	0.0057	0.0097	0.0060	0.0012	0.0006
JPLP	100	bias $\Delta$	-0.0043	0.0023	-0.0004	0.0041	0.0048	0.0003	0.0008
JPLP	10	S.E.	0.0828	0.0573	0.2556	0.1854	0.0992	0.0834	0.0498
JPLP	25	S.E.	0.0512	0.0360	0.1453	0.0960	0.0586	0.0477	0.0288
JPLP	50	S.E.	0.0366	0.0256	0.0999	0.0647	0.0406	0.0334	0.0201
JPLP	75	S.E.	0.0298	0.0208	0.0812	0.0519	0.0331	0.0272	0.0164
JPLP	100	S.E.	0.0258	0.0179	0.0699	0.0442	0.0287	0.0233	0.0141
$\text{PLP} \leftarrow \text{JPLP}$	10	bias $\Delta$	-0.1843		-0.1234	0.1599	0.1923	0.0645	0.0434
$\text{PLP} \leftarrow \text{JPLP}$	25	bias $\Delta$	-0.1740		-0.0866	0.1053	0.1769	0.0514	0.0374
$\text{PLP} \leftarrow \text{JPLP}$	50	bias $\Delta$	-0.1734		-0.0854	0.0977	0.1718	0.0531	0.0355
$\text{PLP} \leftarrow \text{JPLP}$	75	bias $\Delta$	-0.1724		-0.0874	0.0960	0.1686	0.0511	0.0346
$\text{PLP} \leftarrow \text{JPLP}$	100	bias $\Delta$	-0.1713		-0.0811	0.0925	0.1674	0.0512	0.0349
$\text{PLP} \leftarrow \text{JPLP}$	10	S.E.	0.0580		0.2952	0.2078	0.1041	0.0946	0.0559
$\text{PLP} \leftarrow \text{JPLP}$	25	S.E.	0.0354		0.1671	0.1095	0.0609	0.0546	0.0329
$\text{PLP} \leftarrow \text{JPLP}$	50	S.E.	0.0250		0.1167	0.0743	0.0423	0.0383	0.0230
$\text{PLP} \leftarrow \text{JPLP}$	75	S.E.	0.0204		0.0946	0.0601	0.0344	0.0310	0.0186
$\text{PLP} \leftarrow \text{JPLP}$	100	S.E.	0.0177		0.0810	0.0514	0.0297	0.0266	0.0160

<sup>276</sup> When the models were specified correctly, the bias seems converge to 0 as the number of  
<sup>277</sup> drivers increases; the standard errors converge to 0 roughly proportional to the square root

278 of the number of drivers ( $\sqrt{D}$ ), which is consistent with the central limit theorem. When  
279 the models are not specified correctly, there are still a fair amount of bias when the number  
280 of drivers increases and the speed of converging to zero is not consistent with either the  
281 other two correctly specified simulation scenarios or the central limit theorem. The Gelman-  
282 Rubin diagnostic  $\hat{R}$  were all lower than 1.1 and no low effective sample size (ESS) issues  
283 were reported in **Stan**, suggesting that steady posterior distributions were reached while  
284 estimating the parameters of the simulated data sets.

## 285 VI. DISCUSSION

286 In this article, we proposed a Bayesian hierarchical NHPP with PLP intensity function and a  
287 Bayesian hierarchical JPLP to model naturalistic truck driving data. Our motivation comes  
288 from more popular use of naturalistic driving data sets in the recent decade and real-life  
289 truck driving characteristics of multiple segments nested within shifts. The proposed JPLP  
290 accounts for the characteristics of multiple rests within a shift among commercial truck  
291 drivers. Simulation studies showed the consistency of the Bayesian hierarchical estimation  
292 if the models are specified correctly, as well as the persistent bias when the models are not  
293 specified correctly. A case study of 496 commercial truck drivers demonstrates a considerable  
294 amount of variability exist across drivers. Headway and hard brake tend to occur in early  
295 stages while collision mitigation and rolling stability tend to occur in later stages.

296 The models we have studied are based on models that have been widely applied to the  
297 reliability of repairable systems. The NHPP is a model that implies a minimal repair is done  
298 at each failure; that is, the reliability of the system is restored to its condition immediately  
299 before the failure. For the case of repairable systems, the time required for repair is usually

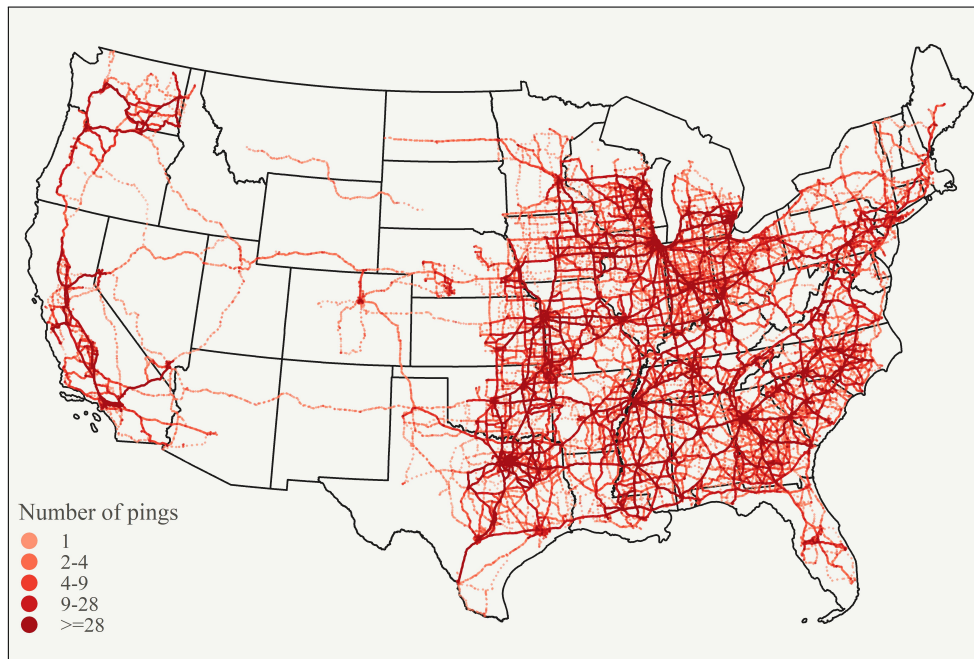
300 not included in the cumulative operating time. In our case, the NHPP implies that the  
301 occurrence of an SCE does not change the intensity of the process. There is no repair  
302 time to account for because the driver continues to drive immediately after the SCE. A rest  
303 break for drivers is analogous to a preventive maintenance for a repairable system whereby a  
304 system's reliability is (possibly) improved by performing the maintenance. Our JPLP model  
305 here is similar to the modulated power law process ((Lakey and Rigdon, 1993; Black and  
306 Rigdon, 1996)), except their model assumed that the reliability might be improved at every  
307 failure/repair.

308 Our models differ in several respects from the repairable systems models. Our models in-  
309 volve the use of covariates, such as weather conditions and driver demographics. In addition,  
310 the heterogeneity of drivers required a hierarchical model. In fact, one important finding is  
311 that driver-to-driver variability accounts for much of the variability of SCEs. Finally, the  
312 size of the data (496 drivers, with over 13 million pings) is much larger than would normally  
313 be encountered in a reliability setting.

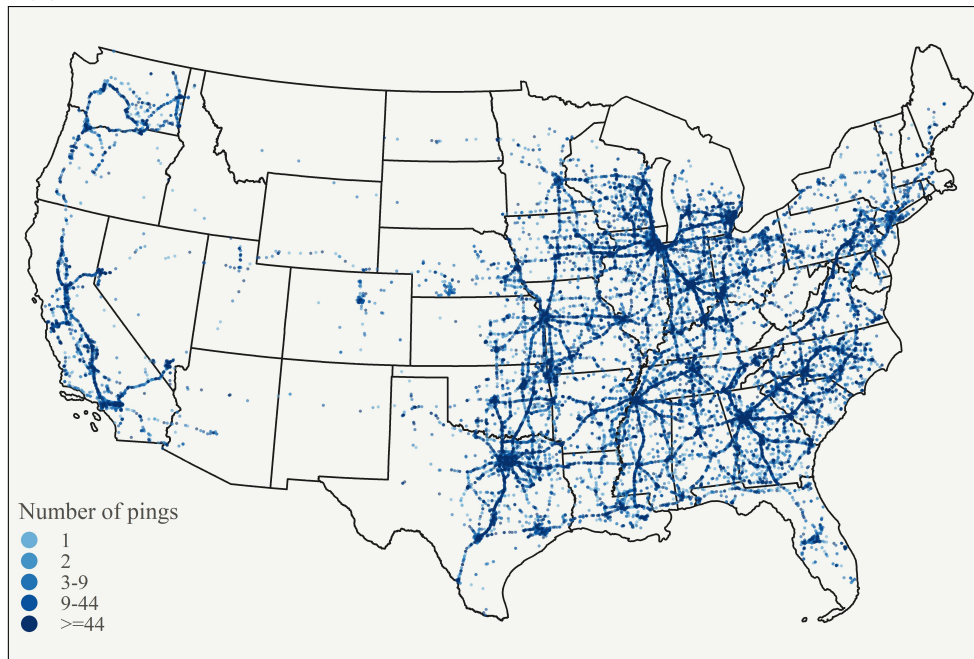
314 From the JASA papers I read, the last paragraph(s) are limitations/future work. So I  
315 would vote for keeping. Our work can be extended in several aspects in the future. First, the  
316 assumption of proportion reliability jump may not hold. Other proper assumptions include  
317 reliability jumping for a fixed-amount jump or jumping dependent on the length of the rest.  
318 Additionally, in our proposed JPLP, the length of breaks within shifts are ignored to simply  
319 the parameterization and likelihood function. In truck transportation practice, longer breaks  
320 certainly have larger effects on reliability jump, hence the relationship between reliability  
321 jump and the length of breaks can have more complex functional forms, so it would be of  
322 interest to test different forms of reliability change as a function of the length of break.

## APPENDICES

324 A. Maps of the naturalistic truck driving study ping data set



(a) Active pings captured from the 496 regional commercial truck drivers.



(b) Inactive pings captured from the 496 regional commercial truck drivers.

Figure 4: Geographical point patterns of active and inactive pings in a large naturalistic commercial truck driving data set.

325 B. Trace plots

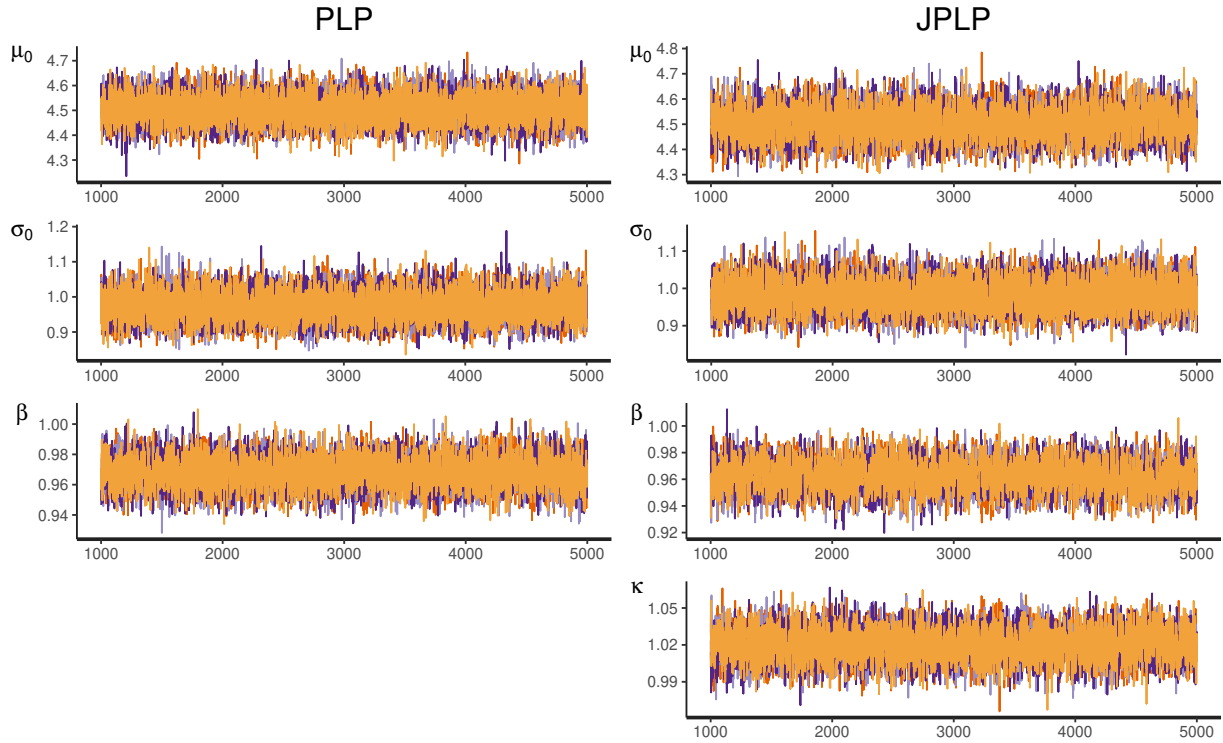


Figure 5: Trace plots of select parameters in PLP (left column) and JPLP (right column) for all types of SCEs

326

## SUPPLEMENTARY MATERIALS

327 Since the real truck driving data provided by our industry partner are confidential and  
 328 cannot be made publicly accessible, we provided a simulated data set that is similar to our  
 329 real data in data structure but has fewer drivers, which means that the computations can be  
 330 completed within a reasonable amount of time. The online supplementary materials contain  
 331 the R code to simulate PLP and JPLP data, explanation on the data structure, and Stan and  
 332 R code for Bayesian hierarchical PLP and JPLP estimation. The supplementary materials  
 333 can be access at <https://for-blind-external-review.github.io/JPLP/>.

334

## ACKNOWLEDGEMENTS

335 The authors are grateful to our industry partner for providing us the naturalistic truck  
336 driving data for research in this study.

337

## FUNDING

338 The fundings are removed here for double-blind peer-review.

339

## REFERENCES

340 Black, S. E. and Rigdon, S. E. (1996). Statistical inference for a modulated power law  
341 process. *Journal of Quality Technology*, 28(1):81–90.

342 Cai, M., Alamdar Yazdi, M. A., Hu, Q., Mehdizadeh, A., Vinel, A., Davis, K. C., Xian,  
343 H., Megahed, F. M., and Rigdon, S. E. (2020). The association between crashes and  
344 safety-critical events: synthesized evidence from crash reports and naturalistic driving data  
345 among commercial truck drivers. *Transportation Research Part C: Emerging Technologies*,

346 Under review.

347 Carpenter, B., Gelman, A., Hoffman, M. D., Lee, D., Goodrich, B., Betancourt, M.,  
348 Brubaker, M., Guo, J., Li, P., and Riddell, A. (2017). Stan: A probabilistic program-  
349 ming language. *Journal of Statistical Software*, 76(1).

350 Das, A., Ghasemzadeh, A., and Ahmed, M. M. (2019). Analyzing the effect of fog weather  
351 conditions on driver lane-keeping performance using the shrp2 naturalistic driving study  
352 data. *Journal of safety research*, 68:71–80.

353 Dingus, T. A., Klauer, S. G., Neale, V. L., Petersen, A., Lee, S. E., Sudweeks, J., Perez,

- 354 M. A., Hankey, J., Ramsey, D., Gupta, S., et al. (2006). The 100-car naturalistic driving  
355 study. phase 2: Results of the 100-car field experiment. Technical report, United States.  
356 Department of Transportation. National Highway Traffic Safety.
- 357 Federal Highway Administration (2019). Human factors. U.S. Department of Transporta-  
358 tion, <https://highways.dot.gov/research/research-programs/safety/human-factors>. [Up-  
359 dated December 2, 2019; accessed July 03, 2020].
- 360 Federal Motor Carrier Safety Administration (2020a). Naturalistic driving study  
361 (data analysis). United States Department of Transportation. [https://www.fmcsa.dot.](https://www.fmcsa.dot.gov/)  
362 gov/research-and-analysis/research/naturalistic-driving-study-data-analysis. [Published  
363 March 10, 2020 and accessed July 03, 2020].
- 364 Federal Motor Carrier Safety Administration (2020b). Summary of hours of service reg-  
365 ulations. United States Department of Transportation. <https://www.fmcsa.dot.gov/>  
366 regulations/hours-service/summary-hours-service-regulations. [Accessed July 03, 2020].
- 367 Gelman, A., Rubin, D. B., et al. (1992). Inference from iterative simulation using multiple  
368 sequences. *Statistical Science*, 7(4):457–472.
- 369 Ghasemzadeh, A. and Ahmed, M. M. (2017). Drivers' lane-keeping ability in heavy rain:  
370 preliminary investigation using shrp 2 naturalistic driving study data. *Transportation*  
371 *research record*, 2663(1):99–108.
- 372 Ghasemzadeh, A. and Ahmed, M. M. (2018). Utilizing naturalistic driving data for in-depth  
373 analysis of driver lane-keeping behavior in rain: Non-parametric mars and parametric

- 374 logistic regression modeling approaches. *Transportation research part C: emerging tech-*  
375 *nologies*, 90:379–392.
- 376 Gordon, T. J., Kostyniuk, L. P., Green, P. E., Barnes, M. A., Blower, D., Blankespoor,  
377 A. D., and Bogard, S. E. (2011). Analysis of crash rates and surrogate events: unified  
378 approach. *Transportation Research Record*, 2237(1):1–9.
- 379 Grove, K., Atwood, J., Hill, P., Fitch, G., DiFonzo, A., Marchese, M., and Blanco, M.  
380 (2015). Commercial motor vehicle driver performance with adaptive cruise control in  
381 adverse weather. *Procedia Manufacturing*, 3:2777–2783.
- 382 Guo, F. (2019). Statistical Methods for Naturalistic Driving Studies. *Annual Review of*  
383 *Statistics and Its Application*, 6:309–328.
- 384 Guo, F., Kim, I., and Klauer, S. G. (2019). Semiparametric Bayesian Models for Evaluating  
385 Time-Variant Driving Risk Factors Using Naturalistic Driving Data and Case-Crossover  
386 Approach. *Statistics in Medicine*, 38(2):160–174.
- 387 Guo, F., Klauer, S. G., Hankey, J. M., and Dingus, T. A. (2010). Near crashes as crash  
388 surrogate for naturalistic driving studies. *Transportation Research Record*, 2147(1):66–74.
- 389 John, S. (2019). 11 incredible facts about the \$700 billion US trucking industry.  
390 Business Insider: Markets Insider. <https://markets.businessinsider.com/news/stocks/trucking-industry-facts-us-truckers-2019-5-1028248577>. [Published online June 3, 2019;  
391 accessed July 03, 2020].
- 393 Kim, S., Chen, Z., Zhang, Z., Simons-Morton, B. G., and Albert, P. S. (2013). Bayesian Hi-

- 394 hierarchical Poisson Regression Models: An Application to a Driving Study With Kinematic  
395 Events. *Journal of the American Statistical Association*, 108(502):494–503.
- 396 Lakey, M. J. and Rigdon, S. E. (1993). Reliability Improvement Using Experimental De-  
397 sign. In *Annual Quality Congress Transactions-American Society for Quality Control*,  
398 volume 47, pages 824–824. American Society for Quality Control.
- 399 Li, Q., Guo, F., Kim, I., Klauer, S. G., and Simons-Morton, B. G. (2018). A Bayesian Finite  
400 Mixture Change-Point Model for Assessing the Risk of Novice Teenage Drivers. *Journal*  
401 *of Applied Statistics*, 45(4):604–625.
- 402 Liu, Y. and Guo, F. (2019). A Bayesian Time-Varying Coefficient Model for Multitype  
403 Recurrent Events. *Journal of Computational and Graphical Statistics*, pages 1–12.
- 404 Liu, Y., Guo, F., and Hanowski, R. J. (2019). Assessing the Impact of Sleep Time on Truck  
405 Driver Performance using a Recurrent Event Model. *Statistics in Medicine*, 38(21):4096–  
406 4111.
- 407 Lord, D. and Mannering, F. (2010). The Statistical Analysis of Crash-Frequency Data: A  
408 Review and Assessment of Methodological Alternatives. *Transportation Research Part A:*  
409 *Policy and Practice*, 44(5):291–305.
- 410 Mannering, F. L. and Bhat, C. R. (2014). Analytic Methods in Accident Research: Method-  
411 ological Frontier and Future Directions. *Analytic Methods in Accident Research*, 1:1–22.
- 412 Mehdizadeh, A., Cai, M., Hu, Q., Yazdi, A., Ali, M., Mohabbati-Kalejahi, N., Vinel, A.,  
413 Rigdon, S. E., Davis, K. C., and Megahed, F. M. (2020). A Review of Data Analytic

- 414 Applications in Road Traffic Safety. Part 1: Descriptive and Predictive Modeling. *Sensors*,  
415 20(4):1107.
- 416 NHTSA's National Center for Statistics and Analysis (2019). 2017 data: large trucks.
- 417 U.S. Department of Transportation. National Highway Traffic Safety Administration.
- 418 Traffic Safety Facts. DOT HS 812 663. <https://crashstats.nhtsa.dot.gov/Api/Public/ViewPublication/812663>. [Published online January 2019; accessed July 03, 2020].
- 419
- 420 Rigdon, S. E. and Basu, A. P. (1989). The Power Law Process: A Model for the Reliability  
421 of Repairable Systems. *Journal of Quality Technology*, 21(4):251–260.
- 422 Rigdon, S. E. and Basu, A. P. (2000). *Statistical Methods for the Reliability of Repairable  
423 Systems*. Wiley New York.
- 424 Savolainen, P. T., Mannerling, F. L., Lord, D., and Quddus, M. A. (2011). The Statistical  
425 Analysis of Highway Crash-injury Severities: A Review and Assessment of Methodological  
426 Alternatives. *Accident Analysis & Prevention*, 43(5):1666–1676.
- 427 Sparrow, A. R., Mollicone, D. J., Kan, K., Bartels, R., Satterfield, B. C., Riedy, S. M.,  
428 Unice, A., and Van Dongen, H. P. (2016). Naturalistic field study of the restart break in  
429 us commercial motor vehicle drivers: truck driving, sleep, and fatigue. *Accident Analysis  
430 & Prevention*, 93:55–64.
- 431 Stan Development Team (2018). RStan: the R interface to Stan. R package version 2.18.2.
- 432 The Dark Sky Company, LLC (2020). Dark Sky API — Overview. <https://darksky.net/dev/docs>. [Online; accessed 20-February-2020].
- 433

<sup>434</sup> The White House (2020). Remarks by President Trump celebrating

<sup>435</sup> America's truckers. [https://www.whitehouse.gov/briefings-statements/](https://www.whitehouse.gov/briefings-statements/remarks-president-trump-celebrating-americas-truckers/)

<sup>436</sup> remarks-president-trump-celebrating-americas-truckers/. [Issued on April 16, 2020;

<sup>437</sup> accessed July 03, 2020].

<sup>438</sup> Tsai, Y.-T., Swartz, S. M., and Megahed, F. M. (2018). Estimating the relative efficiency

<sup>439</sup> of highway safety investments on commercial transportation. *Transportation Journal*,

<sup>440</sup> 57(2):193–218.